p-BaSi₂/n-Si heterojunction solar cells with conversion efficiency reaching 9.0%

Daichi Tsukahara,[1] Suguru Yachi,[1] Hiroki Takeuchi,[1] Ryota Takabe,[1] Weijie Du,[1] Masakazu Baba,[1] Yunpeng Li,[1] Kaoru Toko,[1] Noritaka Usami,[2] and Takashi Suemasu[1]

[1]*Institute of Applied Physics, University of Tsukuba, Tsukuba, Ibaraki 305-8573, Japan*
[2]*Graduate School of Engineering, Nagoya University, Nagoya 464-8603, Japan*

p-BaSi₂/n-Si heterojunction solar cells consisting of a 20 nm thick B-doped p-BaSi₂ epitaxial layer ($p = 2.2 \times 10^{18}$ cm^{-3}) on n-Si(111) ($\rho = 1$–4 Ω cm) were formed by molecular beam epitaxy. The separation of photogenerated minority carriers is promoted at the heterointerface in this structure. Under AM1.5 illumination, the conversion efficiency η reached 9.0%, which is the highest ever reported for solar cells with semiconducting silicides. An open-circuit voltage of 0.46 V, a short-circuit current density of 31.9 mA/cm², and a fill factor of 0.60 were obtained. These results demonstrate the high potential of BaSi₂ for solar cell applications. © 2016 AIP Publishing LLC. [http://dx.doi.org/10.1063/1.4945725]

Crystalline silicon (c-Si) solar cells have been the main-stream of photovoltaics. In 2014, Panasonic Corp. achieved a record energy conversion efficiency η of 25.6% for a hetero-junction with intrinsic thin layer solar cells,[1] and η is approaching the performance limit for c-Si solar cells as determined by their bandgap (E_g). To realize higher efficiency solar cells with lower cost, many studies have been conducted on various thin-film solar cell materials, such as chalcopyrite and cadmium telluride, in efforts to exploit their higher absorption coefficient, α, and more suitable E_g than c-Si.[2–7] Thin-film Si solar cells have also been studied extensively to achieve higher η with the use of efficient light-trapping systems;[8–18] however, it is difficult to obtain η as high as 20%. Thus, the exploration of alternative materials for thin-film solar cell applications is very important. Among such materials, we have focused on semiconducting BaSi₂. BaSi₂ is an indirect bandgap semiconductor with $E_g = 1.3$ eV.[19,20] This value is based on the optical absorption edge of BaSi₂ films we formed. It is also consistent with a recent first-principles calculation using the Heyd–Scuseria–Ernzerhof screened hybrid functional[21] and photon energies obtained from photo-response measurements, above which the photoresponsivity of BaSi₂ begins to increase, regardless of the BaSi₂ layer thickness.[22–24] One of the most striking features of this material is that both a large α and large minority-carrier diffusion length, L, can be utilized. This facilitates the collection of photogenerated carriers in an external circuit. α exceeds 3×10^4 cm^{-1} for photon energies higher than 1.5 eV,[20,21,25,26] despite its indirect bandgap nature. The large α is a result of the direct transition, which starts at energies slightly larger than E_g. In addition, L is as large as approximately 10 μm in undoped n-BaSi₂, which is much larger than its grain size of approximately 0.2 μm.[27] Thus, α and L are sufficiently large for thin-film solar cell applications. We can expect η to be larger than 25% only in a 2 μm thick BaSi₂ pn junction diode.[28] Impurity doping of BaSi₂ with group-III or group-V elements enables control of the carrier type and carrier concentration. For example, the hole concentration, p, can be controlled in a wide range between 10^{16} and 10^{19} cm^{-3} by

boron (B) doping.[29,30] A pn homojunction diode is the most straightforward structure of a solar cell. However, we have only limited information regarding the electrical and optical properties of p-BaSi₂ in contrast to those of undoped n-BaSi₂. A p-BaSi₂/n-Si heterojunction diode would be a suitable configuration to assess the quality of p-BaSi₂ and the potential of BaSi₂ for thin-film solar cell applications because the device structure is quite simple and there is no barrier height at the heterointerface for the transport of photogenerated minority carriers, as discussed later.

According to our previous study, the activation rate of B in BaSi₂ by molecular beam epitaxy (MBE) was only around 10^{-3} when the substrate temperature, T_S, was 600 °C.[30] This is probably because the B concentration, N_B, in the layer was too large at more than 10^{20} cm^{-3}. This assumption was supported by the fact that the B precipitates in the B-doped BaSi₂ layers, as observed using transmission electron microscopy (TEM).[30,31] Such precipitates in B-doped p-BaSi₂ could degrade the solar cell performance. Therefore, in this study, we first aimed to lower the temperature of the B Knudsen cell crucible, T_B, from that in our previous studies to reduce N_B and then investigated the dependence of the activation rate on T_B to find an appropriate T_B. We next adopted the optimum T_B and fabricated p-BaSi₂ (20 nm)/n-Si heterojunction solar cells by MBE, whereby η reached 9.0%, which is approximately 100 times larger than those ever reported for BaSi₂ solar cells[24,32] and is much higher than any other solar cell consisting of semiconducting silicides.[33,34]

An ion-pumped MBE system equipped with an electron-beam evaporation source for Si as well as standard Knudsen cells for Ba and B was used in this investigation. To investigate the activation rate of B atoms doped in BaSi₂, 200 nm thick p-BaSi₂ epitaxial films were formed on high-resistivity n-Si(111) ($\rho > 1000$ Ω cm) substrates at $T_S = 600$ °C with T_B varied from 1200 °C to 1500 °C. Amorphous Si (a-Si) capping layers with thicknesses of a few nanometers were formed on all samples at $T_S < 200$ °C to prevent oxidation of the BaSi₂ surface and to passivate the BaSi₂ surface. Microwave-detected photoconductivity decay measurements

showed that the minority-carrier lifetime reached approximately 10 μs with excellent repeatability for undoped n-BaSi$_2$ by capping the BaSi$_2$ surface with the native oxide or the a-Si layer.[35] However, the barrier height of the native oxide/undoped n-BaSi$_2$ interface for the minority-carriers (holes) in n-BaSi$_2$ is 3.9 eV.[36] Therefore, the transport of holes generated under solar radiation is blocked at the interface, which results in a limited conversion efficiency of $\eta \approx 0.1\%$ for a solar cell with the native oxide/n-BaSi$_2$ interface.[24] For this reason, a-Si was selected as a capping layer in this work. N_B was determined from secondary ion mass spectrometry (SIMS) measurements for several samples. p was measured at temperatures around 22 $^\circ$C by the van der Pauw method for other samples. The details of the growth procedure have been reported previously.[30] For p-BaSi$_2$/n-Si solar cells, T_B was set to 1230 $^\circ$C, and a 20 nm thick B-doped p-BaSi$_2$ epitaxial layer was formed on n-Si(111) ($\rho = 1$–4 Ω cm) at $T_S = 600$ $^\circ$C, followed by a 4 nm thick a-Si capping layer (sample A). For comparison, a sample without the a-Si capping layer was prepared (sample B). Finally, 1 mm diameter and 70 nm thick indium tin oxide (ITO) electrodes were sputtered on the front surface and Al electrodes were deposited on the backside of the n-Si substrate.

The crystalline quality of the grown films was characterized using reflection high-energy electron diffraction (RHEED) and X-ray diffraction (XRD) with Cu Kα radiation. Cross-sections of the samples were observed using TEM (Hitachi, H-9000NAR) with an acceleration voltage of 300 kV. Current density versus voltage (J-V) curves were measured under standard AM1.5, 100 mW/cm^2 illumination at 25 $^\circ$C. Photoresponse and reflectance spectra were also evaluated at this temperature using a lock-in technique with a xenon lamp and a 25 cm focal-length single monochromator (Bunko Keiki, SM-1700A and RU-60N). The light intensity was calibrated with a pyroelectric sensor (Melles Griot, 13PEM001/J). White-bias light was not used. All measurements were performed using a mask with 1 mm diameter holes.

Figure 1 shows Arrhenius plots of N_B ($\bullet$) and p ($\square$). SIMS measurements revealed that as T_B increases, N_B increases exponentially with an activation energy $E_a \approx 6.2$ eV. p measured for three samples of B-doped BaSi$_2$ layers grown at $T_B = 1230$, 1300, and 1400 $^\circ$C were 2.2×10^{18}, 5.0×10^{18}, and 2.0×10^{18} cm^{-3}, respectively. Note that the activation rate of B atoms is close to 1 for B-doped p-BaSi$_2$ formed at $T_B = 1230$ $^\circ$C. Therefore, this T_B was selected for the fabrication of p-BaSi$_2$/n-Si solar cells.

Figure 2(a) shows a θ–2θ XRD pattern for sample A, and the inset shows a streaky RHEED pattern taken for sample A after growth of the p-BaSi$_2$ layer. The diffraction peaks were observed only from the (100) oriented BaSi$_2$ planes, such as (200), (400), and (600), which indicates that the a-axis-oriented B-doped BaSi$_2$ epitaxial film was formed. Figure 2(b) shows a bright-field cross-sectional TEM image of sample A, a-Si (4 nm)/B-doped p-BaSi$_2$ (20 nm)/ n-Si(111). Both the a-Si/BaSi$_2$ and BaSi$_2$/n-Si interfaces are very clear and there are no B precipitations observed in the BaSi$_2$ layer.

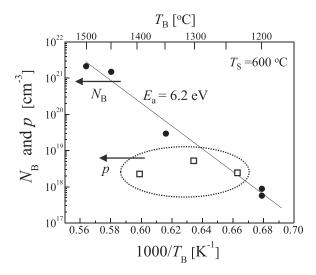Before investigation of the solar cell properties, we describe the expected band alignment of the pn junction

FIG. 1. Arrhenius plots of B concentration (N_B, $\bullet$) and hole concentration (p, $\square$) measured for B-doped BaSi$_2$ layers grown at $T_S = 600$ $^\circ$C. The activation energy, E_a, was 6.2 eV. The ratio of p/N_B is close to 1 for the sample grown at $T_B = 1230$ $^\circ$C.

diode shown in Fig. 3. The hole concentration of the p-BaSi$_2$ was measured to be 2.2×10^{18} cm^{-3}, which is much larger than the electron concentration of n-Si ($n \approx 2 \times 10^{15}$ cm^{-3}). Hence, the depletion region stretches in the n-Si region. The electron affinities of BaSi$_2$ and Si are $q\chi_{BaSi_2} = 3.2$ eV

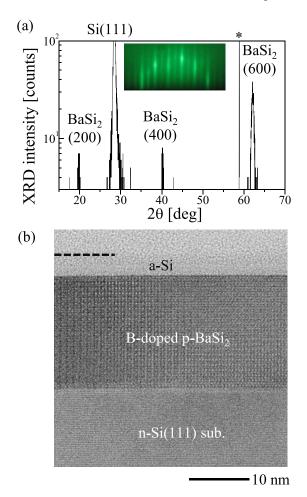FIG. 2. (a) θ-2θ XRD and RHEED patterns for sample A. RHEED was observed along Si[11$\bar{2}$] after the growth of p-BaSi$_2$. The asterisk (*) indicates the peak for the Si substrate used. (b) Cross-sectional TEM image of sample A, a-Si(4 nm)/p-BaSi$_2$ (20 nm)/n-Si heterojunction.
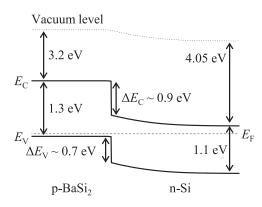
FIG. 3. Expected band alignment of the p-BaSi$_2$/n-Si heterojunction. Due to the difference in the carrier concentration between the p-BaSi$_2$ ($p = 2.2 \times 10^{18}$ cm^{-3}) and n-Si ($n \approx 2 \times 10^{15}$ cm^{-3}) in sample A, the depletion region stretches in the n-Si region.

(Ref. [37]) and $q\chi_{Si} = 4.05$ eV, respectively, and their bandgaps are $E_{g,BaSi_2} = 1.3$ eV and $E_{g,Si} = 1.1$ eV. There is a conduction band offset $\Delta E_C = 4.05 - 3.2 \approx 0.9$ eV and a valence band offset $\Delta E_V = (4.05 + 1.1) - (3.2 + 1.3) \approx 0.7$ eV at the heterointerface. Assuming that the effective density of states at the conduction band of Si, N_C^{Si}, is 2.8×10^{19} cm^{-3}, and that at the valence band of BaSi$_2$, $N_V^{BaSi_2}$, is 2.0×10^{19} cm^{-3},[25] the built-in potential, V_D, is calculated by

$$
\begin{aligned}
V_D &= \left(E_{g,BaSi_2} + q\chi_{BaSi_2} - k_B T \ln\left(\frac{N_V^{BaSi_2}}{p} \right) \right) \Big/ q \\
&\quad - \left(q\chi_{Si} + k_B T \ln\left(\frac{N_C^{Si}}{n} \right) \right) \Big/ q \\
&= (1.3 + 3.2 - 0.06) - (4.05 + 0.25) \approx 0.1 \text{ V}. \quad (1)
\end{aligned}
$$

Here, q is the elemental charge and k_B is the Boltzmann constant. The depletion region widths in the p- and n-layers are estimated to be approximately 3 and 110 nm, respectively, by considering the permittivity of BaSi$_2$, ε_{BaSi_2}, which is 14,[25,38] and that of Si, ε_{Si}, which is 11.9 for photon energies much smaller than their bandgaps. The band offsets ΔE_C and ΔE_V in Fig. 3 promote the separation of photogenerated electrons and holes in p-BaSi$_2$, as well as those in n-Si, which leads to the operation of a solar cell. Therefore, we anticipate that BaSi$_2$ is useful as a hole selective contact for c-Si solar cells. At present, there is insufficient data to discuss the band alignment of the a-Si/p-BaSi$_2$ interface, so that the a-Si layer is excluded in Fig. 3.

Figure 4(a) shows *J-V* curves under AM1.5 illumination for the two samples: sample A capped with the a-Si layer and sample B without the a-Si capping layer. Sample A showed $\eta = 9.0\%$, a short-circuit current density J_{SC} of 31.9 mA/cm^2 and an open-circuit voltage V_{OC} of 0.46 V. This efficiency is the largest among those ever reported for solar cells using semiconducting silicides. In contrast, the solar cell performance was degraded for sample B with $\eta = 0.2\%$, $V_{OC} = 0.14$ V, and $J_{SC} = 14.6$ mA/cm^2. To investigate what happened in the diodes, the *J-V* curves were fitted using the following equation:

$$
J = J_0 \left[\exp\left\{ \frac{q(V - SJR_S)}{\gamma k_B T} \right\} - 1 \right] + J_{SC} + \frac{V - SJR_S}{R_{SH}}, \quad (2)
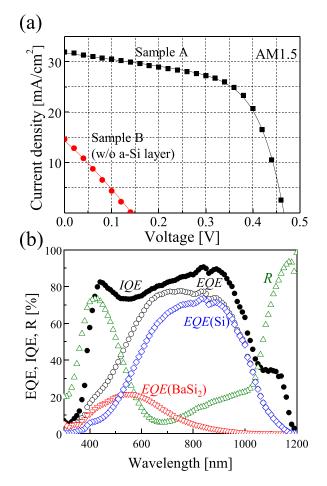$$

FIG. 4. (a) *J-V* characteristics under AM1.5 illumination measured for samples A and B. p-BaSi$_2$ was not capped with a-Si in sample B. (b) *IQE*, *EQE*, and *R* spectra for sample A. The *EQE* spectrum was resolved into contributions from the p-BaSi$_2$ layer, *EQE*(BaSi$_2$), and the n-Si substrate, *EQE*(Si), using the absorption coefficients of BaSi$_2$.

where J_0 is the reverse-bias saturation current density, S is the device area, R_S and R_{SH} are the series resistance and shunt resistance, respectively, and γ is the diode ideality factor. Parameters including a fill factor (*FF*) obtained by the fitting are shown in Table I. In all of the *J-V* characteristics, the data points represent the measured data and solid lines represent the fitted curves using Eq. (2).

We first discuss the effect of the a-Si capping layer on the solar cell performance. According to our previous studies,[35] the a-Si capping layer suppresses oxidation of the surface and behaves as a surface passivation layer. This was confirmed by the minority-carrier lifetime, which reached up to approximately 10 μs with excellent repeatability in undoped n-BaSi$_2$ by capping with a few nanometers thick a-Si layer. An approximately 8 nm thick native oxide layer is formed on BaSi$_2$[36] if the bare BaSi$_2$ is exposed to air, and this layer blocks the carrier transport.[24] The main difference between the two samples is J_0; specifically, J_0 is three orders of magnitude smaller for sample A compared to sample B. In addition, J_{SC} is larger for sample A. It is thus reasonable for V_{OC} to become larger for sample A than for sample B because, in an ideal case, V_{OC} is given by

$$
V_{OC} = \frac{k_B T}{q} \exp\left(1 + \frac{J_{SC}}{J_0} \right). \quad (3)
$$

TABLE I. Solar cell properties for samples A and B are specified.

Sample	a-Si (nm)	J_{SC} (mA/cm^2)	J_0 (mA/cm^2)	V_{OC} (V)	R_S (Ω)	R_{SH} (Ω)	FF	γ	Efficiency (%)
A	4	31.9	3.1×10^{-4}	0.46	50	9830	0.60	1.59	9.0
B	0	14.6	6.0×10^{-1}	0.14	879	6866	0.25	1.57	0.2

Therefore, the formation of a-Si capping layer is a very effective means to improve the solar cell performance.

Next, we discuss the contribution of p-BaSi$_2$ and the n-Si substrate to the measured J_{SC}. Figure 4(b) shows spectra for the internal quantum efficiency (*IQE*), external quantum efficiency (*EQE*), and reflectance (*R*). The *EQE* is resolved into the contribution of BaSi$_2$, *EQE*(BaSi$_2$), and that of Si, *EQE*(Si), using Eqs. (4) and (5)

$$EQE(\text{BaSi}_2) = EQE \times (1 - e^{-\alpha d}), \qquad (4)$$

$$EQE(\text{Si}) = EQE - EQE(\text{BaSi}_2). \qquad (5)$$

Here, α is the wavelength-dependent absorption coefficient of BaSi$_2$[20] and d is 20 nm, the layer thickness of p-BaSi$_2$. The contribution of photogenerated electrons in the p-BaSi$_2$ layer to J_{SC}, i.e., the area ratio of the *EQE*(BaSi$_2$) spectrum to the *EQE* spectrum in Fig. 4(b), was calculated to be 18%; therefore, the remaining 82% was caused by photogenerated holes in the n-Si substrate. Note that the contribution of *EQE*(BaSi$_2$) is distinct, even for such a thin (20 nm) BaSi$_2$ layer. This is attributed to the large absorption coefficients of BaSi$_2$, which are comparable to those of chalcopyrites.[21] This result also clearly demonstrates that the p-BaSi$_2$/n-Si heterointerface does not hinder the transport of photogenerated electrons in p-BaSi$_2$ to the n-Si side, and photogenerated holes in n-Si migrate to the p-BaSi$_2$ side as expected in Fig. 3. There are many other approaches to improve η even further, e.g., making J_0 much smaller, which would result in a larger V_{OC}. At present, we do not have sufficient data to discuss the causes for the large J_0, but we speculate that it is due to defects at the p-BaSi$_2$/n-Si heterointerface. In addition, R should be suppressed, especially for wavelengths around 400 nm and 1100 nm, as shown in Fig. 4(b). R_S should also be reduced much further to improve the *FF*. *EQE*(BaSi$_2$) could be increased with a thicker p-BaSi$_2$ layer. Based on the present results, we conclude that BaSi$_2$ is an attractive material for thin-film solar cell applications.

In summary, B-doped p-BaSi$_2$ films were formed by MBE, and an activation rate of B atoms close to 1 was achieved at temperatures around 22 °C for a sample grown at $T_B = 1230$ °C and $T_S = 600$ °C. TEM observations indicated that no B precipitates were present in the film. p-BaSi$_2$/n-Si solar cells were then fabricated with a 20 nm thick B-doped p-BaSi$_2$ epitaxial film using MBE and the potential of BaSi$_2$ for thin-film solar cell applications was assessed. η was improved significantly by capping the p-BaSi$_2$ surface with a 4 nm thick a-Si layer. The device showed $\eta = 9.0\%$ with $V_{OC} = 0.46$ V, $J_{SC} = 31.9$ mA/cm^2, and $FF = 0.60$. This is the highest η ever reported for solar cells fabricated with semiconducting silicides. The contribution of p-BaSi$_2$ to the measured J_{SC} was estimated to be 18%.

[1]K. Masuko, M. Shigematsu, T. Hashiguchi, D. Fujishima, M. Kai, N. Yoshimura, T. Yamaguchi, Y. Ichihashi, T. Mishima, N. Matsubara, T. Yamanishi, T. Takahama, M. Taguchi, E. Maruyama, and S. Okamoto, IEEE J. Photovoltaics **4**, 1433 (2014).

[2]A. Romeo, A. Terheggen, D. Abou-Ras, D. L. Batzner, F. J. Haug, M. Kalin, D. Rudmann, and A. N. Tiwari, Prog. Photovoltaics **12**, 93 (2004).

[3]I. Repins, M. A. Contreras, B. Egaas, C. DeHart, J. Scharf, C. L. Perkins, B. To, and R. Noufi, Prog. Photovoltaics **16**, 235 (2008).

[4]M. A. Green and S. R. Wenham, Appl. Phys. Lett. **65**, 2907 (1994).

[5]H. Katagiri, K. Jimbo, W. S. Maw, K. Oishi, M. Yamazaki, H. Araki, and A. Takeuchi, Thin Solid Films **517**, 2455 (2009).

[6]K. Tanaka, M. Oonuki, N. Moritake, and H. Uchiki, Sol. Energy Mater. Sol. Cells **93**, 583 (2009).

[7]W. W. Yu, L. Qu, W. Guo, and X. Peng, Chem. Mater. **15**, 2854 (2003).

[8]R. G. Gordon, J. Proscia, F. B. Ellis, Jr., and A. E. Delahoy, Sol. Energy Mater. **18**, 263 (1989).

[9]P. Campbell, Sol. Energy Mater. **21**, 165 (1990).

[10]H. Sasaki, H. Morikawa, Y. Matsuno, M. Deguchi, T. Ishihara, H. Kumabe, T. Murotani, and S. Mitsui, Jpn. J. Appl. Phys., Part 1 **33**, 3389 (1994).

[11]J. Meier, S. Dubail, R. Platz, P. Torres, U. Kroll, J. A. A. Selvan, N. P. Vaucher, Ch. Hof, D. Fischer, H. Keppner, R. Flückiger, A. Shah, V. Shklover, and K.-D. Ufert, Sol. Energy Mater. Sol. Cells **49**, 35 (1997).

[12]O. Vetterl, F. Finger, R. Carius, P. Hapke, L. Houben, O. Kluth, A. Lambertz, A. Mück, B. Rech, and H. Wagner, Sol. Energy Mater. Sol. Cells **62**, 97 (2000).

[13]A. Poruba, A. Fejfar, Z. Remes, J. Springer, M. Vanecek, and J. Kocka, J. Appl. Phys. **88**, 148 (2000).

[14]J. Müller, B. Rech, J. Springer, and M. Vanecek, Sol. Energy **77**, 917 (2004).

[15]M. Berginski, J. Hüpkes, M. Schulte, G. Schöpe, H. Stiebig, and B. Rech, J. Appl. Phys. **101**, 074903 (2007).

[16]D. Zhou and R. Biswas, J. Appl. Phys. **103**, 093102 (2008).

[17]A. Hongsingthong, T. Krajangsang, I. A. Yunaz, S. Miyajima, and M. Konagai, Appl. Phys. Express **3**, 051102 (2010).

[18]H. Sai, Y. Kanamori, and M. Kondo, Appl. Phys. Lett. **98**, 113502 (2011).

[19]K. Morita, Y. Inomata, and T. Suemasu, Thin Solid Films **508**, 363 (2006).

[20]K. Toh, T. Saito, and T. Suemasu, Jpn. J. Appl. Phys., Part 1 **50**, 068001 (2011).

[21]M. Kumar, N. Umezawa, and M. Imai, Appl. Phys. Express **7**, 071203 (2014).

[22]W. Du, M. Suzuno, M. Ajmal Khan, K. Toh, M. Baba, K. Nakamura, K. Toko, N. Usami, and T. Suemasu, Appl. Phys. Lett. **100**, 152114 (2012).

[23]S. Koike, K. Toh, M. Baba, K. Toko, K. O. Hara, N. Usami, N. Saito, N. Yoshizawa, and T. Suemasu, J. Cryst. Growth **378**, 198 (2013).

[24]W. Du, R. Takabe, M. Baba, H. Takeuchi, K. O. Hara, K. Toko, N. Usami, and T. Suemasu, Appl. Phys. Lett. **106**, 122104 (2015).

[25]D. B. Migas, V. L. Shaposhnikov, and V. E. Borisenko, Phys. Status Solidi B **244**, 2611 (2007).

[26]M. Kumar, N. Umezawa, and M. Imai, J. Appl. Phys. **115**, 203718 (2014).

[27]M. Baba, K. Toh, K. Toko, N. Saito, N. Yoshizawa, K. Jiptner, T. Sakiguchi, K. O. Hara, N. Usami, and T. Suemasu, J. Cryst. Growth **348**, 75 (2012).

[28]T. Suemasu, Jpn. J. Appl. Phys., Part 1 **54**, 07JA01 (2015).

[29]M. Ajmal Khan, K. O. Hara, W. Du, M. Baba, K. Nakamura, M. Suzuno, K. Toko, N. Usami, and T. Suemasu, Appl. Phys. Lett. **102**, 112107 (2013).

[30]M. A. Khan, K. Nakamura, W. Du, K. Toko, N. Usami, and T. Suemasu, Appl. Phys. Lett. **104**, 252104 (2014).

[31]D. Tsukahara, M. Baba, S. Honda, Y. Imai, K. O. Hara, N. Usami, K. Toko, J. H. Werner, and T. Sueamsu, J. Appl. Phys. **116**, 123709 (2014).

[32]A. Sasaki, Y. Kataoka, K. Aoki, S. Saito, K. Kobayashi, T. Ito, K. Kakushima, and H. Iwai, Jpn. J. Appl. Phys., Part 1 **54**, 031202 (2015).

[33]Z. Liu, S. Wang, N. Otogawa, Y. Suzuki, M. Osamura, Y. Fukuzawa, T. Ootsuka, Y. Nakayama, H. Tanoue, and Y. Makita, Sol. Energy Mater. Sol. Cells **90**, 276 (2006).

[34]G. K. Dalapati, S. Masudy-Panah, A. Kumar, C. C. Tan, H. R. Tan, and D. Chi, Sci. Rep. **5**, 17810 (2015).

[35]R. Takabe, K. O. Hara, M. Baba, W. Du, N. Shimada, K. Toko, N. Usami, and T. Suemasu, J. Appl. Phys. **115**, 193510 (2014).

[36]R. Takabe, W. Du, K. Ito, H. Takeuchi, K. Toko, S. Ueda, A. Kimura, and T. Suemasu, J. Appl. Phys. **119**, 025306 (2016).

[37]T. Suemasu, K. Morita, M. Kobayashi, M. Saida, and M. Sasaki, Jpn. J. Appl. Phys., Part 2 **45**, L519 (2006).

[38]N. A. Latiff, T. Yoneyama, T. Shibutami, K. Matsumaru, K. Toko, and T. Suemasu, Phys. Status Solidi C **10**, 1759 (2013).